

SEARCHING FOR NEW PHYSICS WITH CHARM * †

J.L. HEWETT

Stanford Linear Accelerator Center, Stanford University, Stanford, CA 94309, USA

ABSTRACT

We consider the prospect of using the charm system as a laboratory for probing new physics. The theoretical expectations for rare charm meson decays, $D^0 - \bar{D}^0$, and charm quark asymmetries in Z decays are examined in the Standard Model. The effects of new physics from several classes of non-standard dynamical models are summarized for these phenomena.

1. Overview

One of the outstanding problems in particle physics is the mysterious origin of the fermion mass and mixing spectrum. One approach in addressing this question is to perform a detailed study of the properties of all fermions. While investigations of the K and B systems have and will continue to play a central role in our quest to understand flavor physics, in-depth examinations of the charm-quark sector have yet to be performed, leaving a gap in our knowledge. Since charm is the only heavy charged $+2/3$ quark presently accessible to experiment, it provides the sole window of opportunity to examine flavor physics in this sector. In addition, charm allows a complimentary probe of Standard Model (SM) physics and beyond to that attainable from the down-quark sector.

Due to the effectiveness of the GIM mechanism, short distance SM contributions to rare charm processes are very small. Most reactions are thus dominated by long range effects which are difficult to reliably calculate. However, for some interactions, there exists a window for the potential observation of new physics. In fact, it is precisely because the SM flavor changing neutral current (FCNC) rates are so small that charm provides an untapped opportunity to discover new effects and offers a detailed test of the SM in the up-quark sector. In this talk, we first review the expectations for rare D meson decays, focusing on radiative charm decays. We next discuss $D^0 - \bar{D}^0$ mixing, first in the SM, then in a variety of models with new interactions. We then finish with a summary of new physics effects in charm quark asymmetries in Z decays.

2. Rare Decays of Charm

FCNC decays of charm mesons include the processes $D^0 \rightarrow \ell^+ \ell^-$, $\gamma\gamma$, and $D \rightarrow X_u + \gamma$, $X_u + \nu\bar{\nu}$, $X_u + \ell^+ \ell^-$, with $\ell = e, \mu$. They proceed via electromagnetic or weak

*Work Supported by the Department of Energy, Contract DE-AC03-76SF00515

†Presented at *Lafex International School on High Energy Physics (LISHEP95)*, Rio de Janeiro, Brazil, February 6-22, 1995

Decay Mode	Experimental Limit	$B_{S,D}$	$B_{L,D}$
$D^0 \rightarrow \mu^+ \mu^-$	$< 1.1 \times 10^{-5}$	$(1 - 20) \times 10^{-19}$	$< 3 \times 10^{-15}$
$D^0 \rightarrow e^+ e^-$	$< 1.3 \times 10^{-4}$		
$D^0 \rightarrow \mu^\pm e^\mp$	$< 1.0 \times 10^{-4}$	0	0
$D^0 \rightarrow \gamma\gamma$	—	10^{-16}	$< 3 \times 10^{-9}$
$D \rightarrow X_u + \gamma$		$(4 - 8) \times 10^{-12}$	
$D^0 \rightarrow \rho^0 \gamma$	$< 1.4 \times 10^{-4}$		$(1 - 5) \times 10^{-6}$
$D^0 \rightarrow \phi^0 \gamma$	$< 2.0 \times 10^{-4}$		$(0.1 - 3.4) \times 10^{-5}$
$D \rightarrow X_u + \ell^+ \ell^-$		4×10^{-9}	
$D^0 \rightarrow \pi^0 \mu \mu$	$< 1.7 \times 10^{-4}$		
$D^0 \rightarrow \bar{K}^0 ee / \mu \mu$	$< 17.0/2.5 \times 10^{-4}$		$< 2 \times 10^{-15}$
$D^0 \rightarrow \rho^0 ee / \mu \mu$	$< 2.4/4.5 \times 10^{-4}$		
$D^+ \rightarrow \pi^+ ee / \mu \mu$	$< 250/4.6 \times 10^{-5}$	few $\times 10^{-10}$	$< 10^{-8}$
$D^+ \rightarrow K^+ ee / \mu \mu$	$< 480/8.5 \times 10^{-5}$		$< 10^{-15}$
$D^+ \rightarrow \rho^+ \mu \mu$	$< 5.8 \times 10^{-4}$		
$D^0 \rightarrow X_u + \nu \bar{\nu}$		2.0×10^{-15}	
$D^0 \rightarrow \pi^0 \nu \bar{\nu}$	—	4.9×10^{-16}	$< 6 \times 10^{-16}$
$D^0 \rightarrow \bar{K}^0 \nu \bar{\nu}$	—		$< 10^{-12}$
$D^+ \rightarrow X_u + \nu \bar{\nu}$	—	4.5×10^{-15}	
$D^+ \rightarrow \pi^+ \nu \bar{\nu}$	—	3.9×10^{-16}	$< 8 \times 10^{-16}$
$D^+ \rightarrow K^+ \nu \bar{\nu}$	—		$< 10^{-14}$

Table 1: Standard Model predictions for the branching fractions due to short and long distance contributions for various rare D meson decays. Also shown are the current experimental limits.

penguin diagrams as well as receiving contributions from box diagrams in some cases. The short distance SM contributions to these decays are quite small, as the masses of the quarks which participate inside the loops (d, s, and b) are tiny, resulting in a very effective GIM mechanism. The calculation of the short distance rates for these processes is straightforward and the transition amplitudes and standard loop integrals, which are categorized in Ref. 1 for rare K decays, are easily converted to the D system. The loop integrals relevant for $D^0 \rightarrow \gamma\gamma$ may be found in Ref. 2. Employing the GIM mechanism results in the general expression for the amplitudes,

$$\mathcal{A} \sim V_{cs} V_{us}^* [F(x_s) - F(x_d)] + V_{cb} V_{ub}^* [F(x_b) - F(x_d)], \quad (1)$$

with V_{ij} representing the relevant Cabibbo-Kobayashi-Maskawa (CKM) matrix elements, and $x_i \equiv m_i^2/M_W^2$. The magnitude of the s - and b -quark contributions are generally comparable as the larger CKM factors compensate for the small strange quark mass. The values of the resulting inclusive short distance branching fractions, are summarized in Table 1, along with the current experimental bounds.^{3,4} The corresponding short distance exclusive rates are typically an order of magnitude less than the inclusive case. We note that the transition $D^0 \rightarrow \ell^+ \ell^-$, is helicity suppressed; the

range given for this branching fraction, $(1 - 20) \times 10^{-19}$, indicates the effect of varying the parameters in the ranges $f_D = 0.15 - 0.25$ GeV and $m_s = 0.15 - 0.40$ GeV.

The calculation of the long distance branching fractions are plagued with hadronic uncertainties and the estimates listed in Table 1 convey an upper limit on the size of these effects rather than an actual value. These estimates have been computed by considering various intermediate particle states (*e.g.*, $\pi, K, \bar{K}, \eta, \eta', \pi\pi$, or $K\bar{K}$) and inserting the known rates for the decay of the intermediate particles into the final state of interest. In all cases we see that the long distance contributions overwhelm those from SM short distance physics

The radiative decays, $D \rightarrow X_u + \gamma$, warrant further discussion. Before QCD corrections are applied, the short distance inclusive rate is very small, $B(c \rightarrow u\gamma) = 1.4 \times 10^{-17}$; however, the QCD corrections greatly enhance this rate. These corrections have recently been calculated⁵ employing an operator product expansion, where the effective Hamiltonian is evolved at leading logarithmic order from the electroweak scale down to $\mu \sim m_c$ by the Renormalization Group Equations. The evolution is performed in two successive steps; first from the electroweak scale down to m_b working in an effective 5 flavor theory, and then to $\mu < m_b$ in an effective 4 flavor theory. We note that care must be taken in the operator expansion in order to correctly account for the CKM structure of the operators. This procedure results⁵ in $B(c \rightarrow u\gamma) = (4.21 - 7.94) \times 10^{-12}$, where the lower(upper) value in the numerical range corresponds to the scale $\mu = 2m_c(m_c)$. The effects of the QCD corrections are dramatic, and the rate is almost entirely due to operator mixing. The stability of this result can be tested once the complete next-to-leading order corrections are known.

The long range effects in radiative charm meson decays have also been recently examined in Ref. 5. These effects can be separated into two classes, (i) pole amplitudes, which correspond to the annihilation processes $c\bar{q}_1 \rightarrow q_2\bar{q}_3$ with the photon radiating from any of the quarks, and (ii) vector meson dominance (VMD) contributions, which are described by the underlying process $c \rightarrow q_1\bar{q}_2q$ followed by the conversion $\bar{q}_2q \rightarrow \gamma$. In the first class, either the D meson experiences weak mixing with the particle intermediate states before photon emission occurs (denoted as as type I transition), or the photon is emitted before weak mixing, *i.e.*, the final state meson is created via weak mixing (designated as type II). The case of pseudoscalar intermediate states was considered in the type I amplitudes, since the pseudoscalar-photon-final state meson coupling can be phenomenologically inferred from data. In type II transitions, the $D\gamma D_n^*$ vertices have not yet been experimentally determined and thus one must rely on theoretical modeling. We note that both of these amplitudes are parity conserving due to the electromagnetic transition. In VMD reactions, the amplitudes have been calculated using both (i) a phenomenological approach, which utilizes available data on $D \rightarrow MV$ transitions, and (ii) the theoretical model of Bauer, Stech, and Wirbel.⁶ The expectations for the transition amplitude in each case are presented in Table 2, as well as the resulting range of predicted branching fractions for various exclusive decay modes. We see that there is a wide range of predictions, and that the long range effects completely dominate over the short distance physics. Observation of several of these exclusive decays, would test the theoretical modeling, and would enable the scaling of predictions to the B sector with greater accuracy. This would be important for the case

Mode	\mathcal{A}^{pc}			\mathcal{A}^{pv}	$B(D \rightarrow M\gamma) (10^{-5})$
	P-I	P-II	VMD	VMD	
$D_s^+ \rightarrow \rho^+\gamma$	8.2	-1.9	± 3.2	± 2.8	6 - 38
$D^0 \rightarrow \bar{K}^{*0}\gamma$	5.6	-5.9	± 3.8	$\pm(5.1 - 6.8)$	7 - 12
$D_s^+ \rightarrow b_1^+\gamma$	7.2	—	—	—	~ 6.3
$D_s^+ \rightarrow a_1^+\gamma$	1.2	—	—	—	~ 0.2
$D_s^+ \rightarrow a_2^+\gamma$	2.1	—	—	—	~ 0.1
$D^+ \rightarrow \rho^+\gamma$	1.3	-0.4	± 1.6	± 1.9	2 - 6
$D^+ \rightarrow b_1^+\gamma$	1.2	—	—	—	~ 3.5
$D^+ \rightarrow a_1^+\gamma$	0.5	—	—	—	~ 0.04
$D^+ \rightarrow a_2^+\gamma$	3.4	—	—	—	~ 0.03
$D_s^+ \rightarrow K^{*+}\gamma$	2.8	-0.5	± 0.9	± 1.0	-8 - 3
$D_s^+ \rightarrow K_2^{*+}\gamma$	6.0	—	—	—	~ 0.2
$D^0 \rightarrow \rho^0\gamma$	0.5	-0.5	$\pm(0.2 - 1.0)$	$\pm(0.6 - 1.0)$	0.1 - 0.5
$D^0 \rightarrow \omega^0\gamma$	0.6	-0.7	± 0.6	± 0.7	$\simeq 0.2$
$D^0 \rightarrow \phi^0\gamma$	0.7	-1.6	$\pm(0.6 - 3.5)$	$\pm(0.9 - 2.1)$	0.1 - 3.4
$D^+ \rightarrow K^{*+}\gamma$	0.4	-0.1	± 0.4	± 0.4	0.1 - 0.3
$D^0 \rightarrow K^{*0}\gamma$	0.2	-0.3	± 0.2	± 0.2	$\simeq 0.01$

Table 2: Predictions for the amplitudes (in units of 10^8 GeV^{-1}) and branching fractions of exclusive charm decays due to long distance contributions.

of $B \rightarrow \rho\gamma$, which suffers from long distance uncertainties,⁷ and from which one would like to extract the CKM matrix element V_{td} .

Lepton flavor violating decays, *e.g.*, $D^0 \rightarrow \mu^\pm e^\mp$ and $D \rightarrow X + \mu^\pm e^\mp$, are strictly forbidden in the SM with massless neutrinos. In a model with massive non-degenerate neutrinos and non-vanishing neutrino mixings, such as in four generation models, $D^0 \rightarrow \mu^\pm e^\mp$ would be mediated by box diagrams with the massive neutrinos being exchanged internally. LEP data restricts⁸ heavy neutrino mixing with e and μ to be $|U_{Ne}U_{N\mu}^*|^2 < 7 \times 10^{-6}$ for a neutrino with mass $m_N > 45 \text{ GeV}$. Consistency with this bound constrains⁹ the branching fraction to be $B(D^0 \rightarrow \mu^\pm e^\mp) < 6 \times 10^{-22}$. This result also holds for a heavy singlet neutrino which is not accompanied by a charged lepton. The observation of this decay at a larger rate than the above bound would be a clear signal for the existence of a different class of models with new physics.

Examining Table 1, we see that the SM short distance contributions to rare charm decays are overwhelmed by the long distance effects. The observation of any of these modes at a larger rate than what is predicted from long distance interactions would provide a clear signal for new physics. To demonstrate the magnitude of enhancements that are possible in theories beyond the SM, we consider two examples (i) leptoquark exchange mediating $D^0 \rightarrow \mu^\pm e^\mp$ and (ii) a heavy $Q = -1/3$ quark contributing to $c \rightarrow u\gamma$. Leptoquarks are color triplet particles which couple to a lepton-quark pair and are naturally present in many theories beyond the SM which relate leptons and quarks at a more fundamental level. We parameterize their *a priori* unknown couplings as $\lambda_{lq}^2/4\pi =$

$F_{lq}\alpha$. Leptoquarks can mediate $D^0 \rightarrow \mu^\pm e^\mp$ by tree-level exchange, however their contributions are suppressed by angular momentum conservation. From the present limit $B(D^0 \rightarrow \mu^\pm e^\mp) < 10^{-4}$, Davidson *et al.*¹⁰ derive the bound on the leptoquark mass m_{lq} and coupling,

$$\sqrt{F_{eu}F_{\mu c}} < 4 \times 10^{-3} \frac{\alpha}{4\pi} \left[\frac{m_{lq}}{100\text{GeV}} \right]^2. \quad (2)$$

These constraints surpass those from HERA.¹¹ In the second example of new physics contributions, we examine a heavy $Q = -1/3$ quark, which may be present, *e.g.*, as an iso-doublet fourth generation b' quark, or as a singlet quark in E_6 grand unified theories. The current bound³ on the mass of such an object is $m_{b'} > 85$ GeV, assuming that it decays via charged current interactions. The heavy quark will then participate inside the penguin diagrams which mediate $c \rightarrow u\gamma$, with the appropriate CKM factors. From unitarity considerations, the fourth generation CKM factor will also contribute to the coefficient of the current-current operator which dominates the branching fraction via mixing. The resulting $B(D \rightarrow X_u\gamma)$ is presented in Fig. 1 as a function of the fourth generation CKM mixing factor, for several values of the heavy quark mass. We see that a sizeable enhancement of the three generation short distance rate is possible, however, the short distance rate is still overpowered by the long range effects.

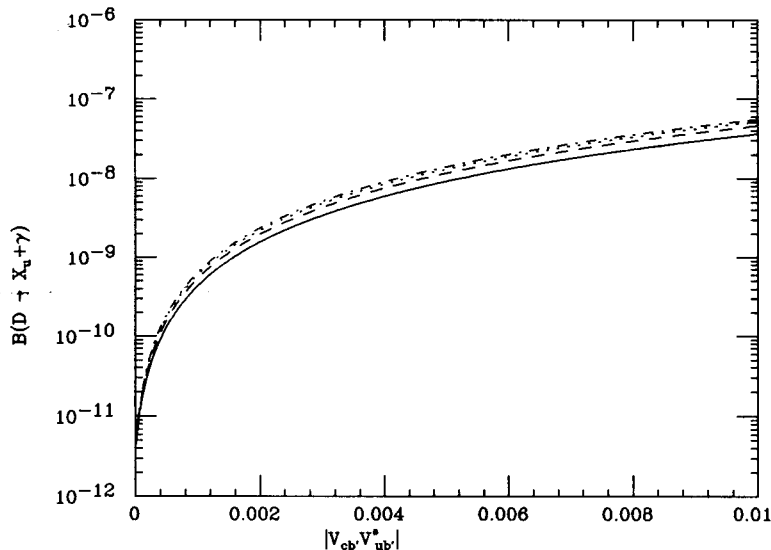


Figure 1: Branching fraction for $D \rightarrow X_u\gamma$ in the four generation SM as a function of the CKM mixing factor, with the solid, dashed, dotted, dash-dotted curve corresponding to $m_{b'} = 100, 200, 300, 400$ GeV, respectively.

Non-SM contributions may also affect the purely leptonic decays $D \rightarrow \ell\nu_\ell$. Signatures for new physics include the measurement of non-SM values for the absolute

branching ratios, or the observation of a deviation from the SM prediction

$$\frac{B(D_{(s)}^+ \rightarrow \mu^+ \nu_\mu)}{B(D_{(s)}^+ \rightarrow \tau^+ \nu_\tau)} = \frac{m_\mu^2 \left(1 - m_\mu^2/m_{D_{(s)}}^2\right)^2}{m_\tau^2 \left(1 - m_\tau^2/m_{D_{(s)}}^2\right)^2}. \quad (3)$$

This ratio is sensitive to violations of $\mu - \tau$ universality.

As another example, we consider the case where the SM Higgs sector is enlarged by an additional Higgs doublet. These models generate important contributions¹² to the decay $B \rightarrow \tau \nu_\tau$ and it is instructive to examine their effects in the charm sector. Two such models, which naturally avoid tree-level flavor changing neutral currents, are Model I, where one doublet (ϕ_2) generates masses for all fermions and the second (ϕ_1) decouples from the fermion sector, and Model II, where ϕ_2 gives mass to the up-type quarks, while the down-type quarks and charged leptons receive their mass from ϕ_1 . Each doublet receives a vacuum expectation value v_i , subject to the constraint that $v_1^2 + v_2^2 = v_{SM}^2$. The charged Higgs boson present in these models will mediate the leptonic decay through an effective four-Fermi interaction, similar to that of the SM W -boson. The H^\pm interactions with the fermion sector are governed by the Lagrangian

$$\mathcal{L} = \frac{g}{2\sqrt{2}M_W} H^\pm [V_{ij} m_{u_i} A_u \bar{u}_i (1 - \gamma_5) d_j + V_{ij} m_{d_j} A_d \bar{u}_i (1 + \gamma_5) d_j + m_\ell A_\ell \bar{\nu}_\ell (1 + \gamma_5) \ell] + h.c., \quad (4)$$

with $A_u = \cot \beta$ in both models and $A_d = A_\ell = -\cot \beta (\tan \beta)$ in Model I(II), where $\tan \beta \equiv v_2/v_1$. In Models I and II, we obtain the result

$$B(D^+ \rightarrow \ell^+ \nu_\ell) = B_{SM} \left(1 + \frac{m_D^2}{m_{H^\pm}^2}\right)^2, \quad (5)$$

where in Model II the D_s^+ decay receives an additional modification

$$B(D_s^+ \rightarrow \ell^+ \nu_\ell) = B_{SM} \left[1 + \frac{m_{D_s}^2}{m_{H^\pm}^2} \left(1 - \tan^2 \beta \frac{m_s}{m_c}\right)\right]^2. \quad (6)$$

In this case, we see that the effect of the H^\pm exchange is independent of the leptonic final state and the above prediction for the ratio in Eq. (3) is unchanged. This is because the H^\pm contribution is proportional to the charged lepton mass, which is then a common factor with the SM helicity suppressed term. However, the absolute branching fractions can be modified; this effect is negligible in the decay $D^+ \rightarrow \ell^+ \nu_\ell$, but could be of order a few percent in D_s^+ decay if $\tan \beta$ is very large.

3. $D^0 - \bar{D}^0$ Mixing

Currently, the limits³ on $D^0 - \bar{D}^0$ mixing are from fixed target experiments, with $x_D \equiv \Delta m_D/\Gamma < 0.083$ (where $\Delta m_D = m_2 - m_1$ is the mass difference), yielding

$\Delta m_D < 1.3 \times 10^{-13}$ GeV. The bound on the ratio of wrong-sign to right-sign final states is $r_D \equiv \Gamma(D^0 \rightarrow \ell^- X)/\Gamma(D^0 \rightarrow \ell^+ X) < 3.7 \times 10^{-3}$, where

$$r_D \approx \frac{1}{2} \left[\left(\frac{\Delta m_D}{\Gamma} \right)^2 + \left(\frac{\Delta \Gamma}{2\Gamma} \right)^2 \right], \quad (7)$$

in the limit $\Delta m_D/\Gamma, \Delta \Gamma/\Gamma \ll 1$. These analyses, however, are based on the assumption that there is no interference between the mixing signal and the dominant background of doubly Cabibbo suppressed decays. It has recently been noted¹³ that while this assumption may be valid for the SM (since the expected size of the mixing is small), it does not necessarily apply in models with new physics where $D^0 - \bar{D}^0$ mixing is potentially large.

The short distance SM contributions to Δm_D proceed through a W box diagram with internal d, s, b -quarks. In this case the external momentum, which is of order m_c , is communicated to the light quarks in the loop and can not be neglected. The effective Hamiltonian is

$$\mathcal{H}_{eff}^{\Delta c=2} = \frac{G_F \alpha}{8\sqrt{2}\pi x_w} \left[|V_{cs}V_{us}^*|^2 \left(I_1^s \mathcal{O} - m_c^2 I_2^s \mathcal{O}' \right) + |V_{cb}V_{ub}^*|^2 \left(I_3^b \mathcal{O} - m_c^2 I_4^b \mathcal{O}' \right) \right], \quad (8)$$

where the I_j^q represent integrals¹⁴ that are functions of m_q^2/M_W^2 and m_q^2/m_c^2 , and $\mathcal{O} \equiv [\bar{u}\gamma_\mu(1 - \gamma_5)c]^2$ is the usual mixing operator while $\mathcal{O}' \equiv [\bar{u}(1 + \gamma_5)c]^2$ arises in the case of non-vanishing external momentum. The numerical value of the short distance contribution is $\Delta m_D \sim 5 \times 10^{-18}$ GeV (taking $f_D = 200$ MeV). The long distance contributions have been computed via two different techniques: (i) the intermediate particle dispersive approach (using current data on the intermediate states) yields¹⁵ $\Delta m_D \sim 10^{-16}$ GeV, and (ii) heavy quark effective theory which results¹⁶ in $\Delta m_D \sim 10^{-17}$ GeV. Clearly, the SM predictions lie far below the present experimental sensitivity! We see that the gap between the short and long distance expectations is not that large, and hence the opportunity exists for new physics to reveal itself.

One reason the SM short distance expectations for $D^0 - \bar{D}^0$ mixing are so small is that there are no heavy particles participating in the box diagram to enhance the rate. Hence the first extension to the SM that we consider is the addition¹⁷ of a heavy $Q = -1/3$ quark. We can now neglect the external momentum and Δm_D is given by the usual expression,¹

$$\Delta m_D = \frac{G_F^2 M_W^2 m_D}{6\pi^2} f_D^2 B_D |V_{cb'}V_{ub'}^*|^2 F(m_{b'}^2/M_W^2). \quad (9)$$

The value of Δm_D is displayed in this model in Fig. 2(a) as a function of the overall CKM mixing factor for various values of the heavy quark mass. We see that Δm_D approaches the current experimental range for large values of the mixing factor.

Next we examine two-Higgs-doublet models discussed above which avoid tree-level FCNC by introducing a global symmetry. The expression for Δm_D in these models can be found in Ref. 18. From the Lagrangian in Eq. (4) it is clear that Model I will only modify the SM result for very small values of $\tan \beta$, and this region is already

excluded^{18,19} from existing data on $b \rightarrow s\gamma$ and $B_d^0 - \bar{B}_d^0$ mixing. However, enhancements can occur in Model II for large values of $\tan\beta$, as demonstrated in Fig. 2(b).

We now consider the case of extended Higgs sectors without natural flavor conservation. In these models the above requirement of a global symmetry which restricts each fermion type to receive mass from only one doublet is replaced²⁰ by approximate flavor symmetries which act on the fermion sector. The Yukawa couplings can then possess a structure which reflects the observed fermion mass and mixing hierarchy. This allows the low-energy FCNC limits to be evaded as the flavor changing couplings to the light fermions are small. We employ the Cheng-Sher ansatz,²⁰ where the flavor changing couplings of the neutral Higgs are $\lambda_{h^0 f_i f_j} \approx (\sqrt{2}G_F)^{1/2} \sqrt{m_i m_j} \Delta_{ij}$, with the $m_{i(j)}$ being the relevant fermion masses and Δ_{ij} representing a combination of mixing angles. h^0 can now contribute to Δm_D through tree-level exchange as well as mediating $D^0 - \bar{D}^0$ mixing by h^0 and t-quark virtual exchange in a box diagram. These latter contributions only compete with those from the tree-level process for large values of Δ_{ij} . In Fig. 2(c-d) we show the value of Δm_D in this model from the tree-level and box diagram contribution, respectively.

The last contribution to $D^0 - \bar{D}^0$ mixing that we will discuss here is that of scalar leptoquark bosons. They participate in Δm_D via virtual exchange inside a box diagram,¹⁰ together with a charged lepton or neutrino. Assuming that there is no leptoquark-GIM mechanism, and taking both exchanged leptons to be the same type, we obtain the restriction

$$\frac{F_{\ell c} F_{\ell u}}{m_{\ell q}^2} < \frac{196\pi^2 \Delta m_D}{(4\pi\alpha f_D)^2 m_D}, \quad (10)$$

where $F_{\ell q}$ is defined in the previous section. The resulting constraints in the leptoquark coupling-mass plane are presented in Fig. 2(e), assuming that a limit of $\Delta m_D < 10^{-13}$ could be obtained from experiment.

4. Charm Quark Asymmetries in Z Decays

The SM continues to provide an excellent description of precision electroweak data,²¹ especially in the light of the discovery of the top-quark²² in the mass range predicted by this data. The only hint of a potential discrepancy is a mere $(2 - 2.5)\sigma$ deviation from SM expectations for the quantity $R_b \equiv \Gamma(Z \rightarrow b\bar{b})/\Gamma(Z \rightarrow \text{hadrons})$. A global fit to all LEP data gives the result²¹ $R_b = 0.2204 \pm 0.0020$. In this fit, the value of R_b is highly correlated to the value of the corresponding quantity R_c , which is measured to be $R_c = 0.1606 \pm 0.0095$. In contrast to the b-quark case, this is in reasonable agreement with the SM expectation of $R_c = 0.171$ (as defined by ZFITTER 4.9²³ with $m_t = 174$ GeV, $m_h = 300$ GeV, and $\alpha_s = 0.125$). The asymmetry parameter, $A_c \equiv 2v_c a_c / (v_c^2 + a_c^2)$, is also measured²¹ at LEP via the charm-quark forward backward asymmetry, $A_{FB}(c) = 0.75 A_e A_c = 0.0760 \pm 0.0089$ and at the SLC via the left-right forward-backward asymmetry $A_{FB}^{LR}(c) = 0.75 A_c$. The SLD value for A_c is²¹ 0.58 ± 0.14 , while the SM predicts²³ 0.668. In the SM, R_b is sensitive to additional vertex corrections involving the top-quark, while the remaining electroweak and QCD radiative corrections largely cancel in the ratio. In contrast, R_c contains no such additional SM vertex corrections.

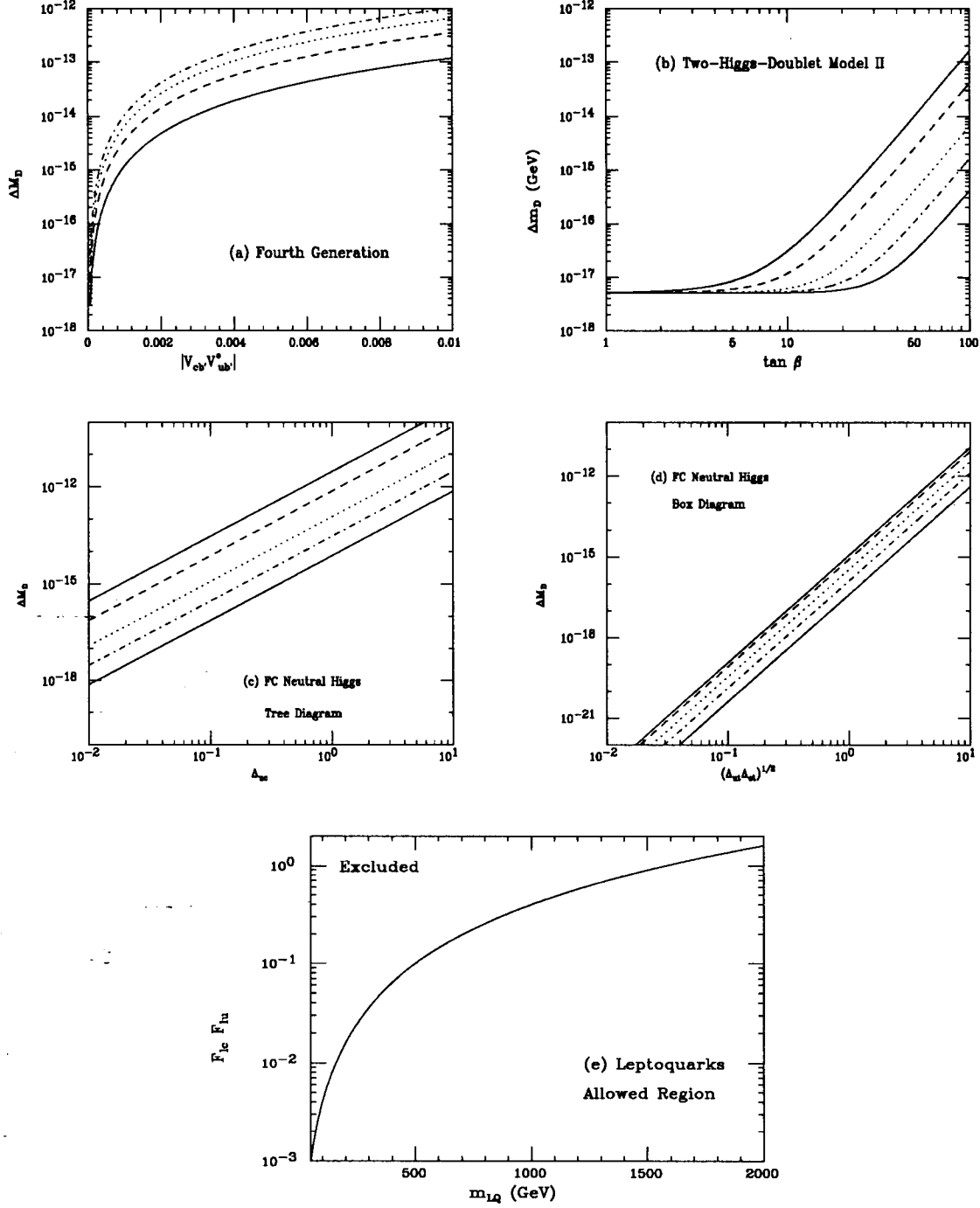


Figure 2: Δm_D in (a) the four generation SM with the same labeling as in Fig. 1, (b) in two-Higgs-doublet model II as a function of $\tan \beta$ with, from top to bottom, the solid, dashed, dotted, dash-dotted, solid curve representing $m_{H^\pm} = 50, 100, 250, 500, 1000$ GeV. The solid horizontal line corresponds to the present experimental limit. (c) Tree-level and (d) box diagrams contributions to Δm_D in the flavor changing Higgs model described in the text as a function of the mixing factor for $m_h = 50, 100, 250, 500, 1000$ GeV corresponding to the solid, dashed, dotted, dash-dotted, and solid curves from top to bottom. (e) Constraints in the leptoquark coupling-mass plane from Δm_D .

The existence of anomalous couplings between the c -quark and the Z boson could cause a significant shift²⁴ in the value of R_c . The lowest dimensional non-renormalizable operators which can be added to the SM take the form of either electric or magnetic dipole form factors. Defining κ and $\tilde{\kappa}$ as the real parts of the magnetic and electric dipole form factors, respectively, (evaluated at $q^2 = M_Z^2$) the interaction Lagrangian is

$$\mathcal{L} = \frac{g}{2c_w} \bar{c} \left[\gamma_\mu (v_b - a_b \gamma_5) + \frac{i}{2m_b} \sigma_{\mu\nu} q^\nu (\kappa_c^Z - i \tilde{\kappa}_c^Z \gamma_5) \right] c Z^\mu. \quad (11)$$

The influence of these couplings on R_c and A_c is presented in Fig. 3(a) from Rizzo,²⁴ where the ratio of these quantities calculated with the above Lagrangian to that of the SM (as defined by ZFITTER²³) is displayed. In this figure the solid (dashed) curves represent the predictions when κ_c^Z ($\tilde{\kappa}_c^Z$) is taken to be non-zero, with the diamonds representing unit steps of 0.002 in these parameters. The position of the data is also shown.

The extended Higgs models without natural flavor conservation discussed above can also affect the $Zc\bar{c}$ vertex. In this case, there is an extra vertex correction due to the exchange of the neutral Higgs and the top-quark. This correction takes the form $(ig/2c_w)(G_F m_t m_c / 8\sqrt{2}\pi^2) \Delta_{ct}^2 \gamma_\mu (v_c \delta v_c - a_c \delta a_c \gamma_5)$, where δv_c and δa_c are given by the loop integrals. The effect of this correction on the asymmetry parameter is shown in Fig. 3(b), where we see that only very large values of Δ_{ct} yield deviations from the SM.

Extended electroweak gauge sectors which contain an extra neutral gauge boson can modify the fermion couplings of the SM Z . These alterations in the couplings arise due to (i) a shift in the values of v_f and a_f due to $Z - Z'$ mixing, (ii) an overall factor of $\sqrt{\rho} = M_Z^{SM}/M_{Z_1}$ due to the shift in the mass of the lightest physical Z_1 , from that predicted in the SM, and (iii) a shift in the value of $x_w = \sin^2 \theta_w$ defined as $x_w(M_{Z_1})$ and not $x_w(M_Z^{SM})$. The variation in the $Z \rightarrow c\bar{c}$ width and in A_c for the extended gauge models based on E_6 and $SO(10)$ grand unified theories²⁵ are shown in Fig. 3(c-d), respectively. In the E_6 case, the solid lines correspond to fixed values of the $Z - Z'$ mixing angle ϕ for a 1 TeV Z' , and the length of the lines represents the variation of the model parameter $-90^\circ \leq \theta_{E_6} \leq 90^\circ$. In the Left-Right Symmetric Model (based on $SO(10)$), A_c is displayed as a function of the ratio of right- to left-handed coupling strength, $\tilde{\kappa} \equiv g_R/g_L$, for various values of the Z' mass.

5. Summary

In summary we see that there is a wide physics potential to motivate an in-depth study of the charm system. We urge our experimental colleagues to study charm with the same precision that has and will be achieved in the down-quark sector.

Acknowledgements

I thank the organizers for providing the opportunity for me to attend this stimulating workshop. I am indebted to my collaborators G. Burdman, E. Golowich, and S. Pakvasa, and I thank T. Rizzo for useful discussions.

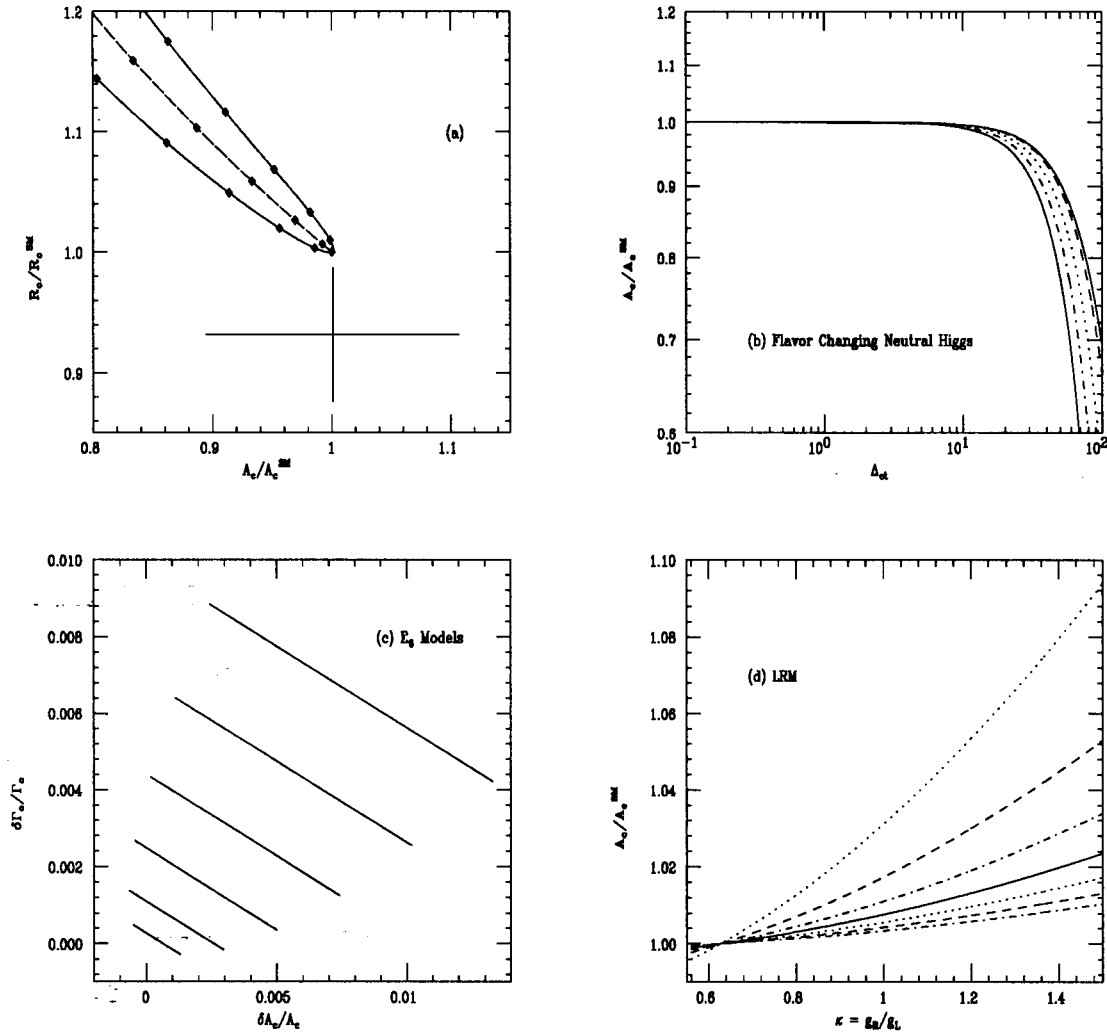


Figure 3: (a) The R_c and A_c plane, scaled to SM predictions, for non-zero values of the electric and magnetic dipole couplings from Rizzo in Ref. 24, where the diamonds represent unit increments in these quantities in steps of 0.002. The error bars represent the data. (b) A_c , scaled to its SM value, in the flavor changing neutral Higgs model as a function of the mixing parameter, for $m_h = 50, 100, 250, 500, 1000$ GeV with the same labeling as in Fig. 2(b). (c) Variations in the $A_c - Zc\bar{c}$ width plane in E_6 models, for $|\phi| = 0.006, 0.005, 0.004, 0.003, 0.002, 0.001$ from top to bottom with a 1 TeV Z' . (d) A_c in the Left-Right Symmetric Model as a function of $\kappa \equiv g_R/g_L$, with a Z' mass of 0.75, 1.0, 1.25, 1.5, 1.75, 2.0, 2.25 TeV corresponding to the dotted, dashed, dashdotted, solid, dotted dashed, dashdotted curves from top to bottom.

References

1. T. Inami and C.S. Lim, *Prog. Theor. Phys.* **65**, 297 (1981).
2. E. Ma and A. Pramudita, *Phys. Rev.* **D24**, 2476 (1981).
3. L. Montanet *et al.*, Particle Data Group, *Phys. Rev.* **D50**, 1173 (1994).
4. M. Selen, CLEO Collaboration, talk presented at *APS Spring Meeting*, Washington D.C., April 1994; J. Cumalet, talk presented at *The Tau-Charm Factory in the Era of B Factories and CESR*, Stanford, CA, August 1994.
5. G. Burdman, E. Golowich, J.L. Hewett, and S. Pakvasa, SLAC Report SLAC-PUB-6692 (1994).
6. M. Bauer, B. Stech, and M. Wirbel, *Z. Phys.* **C29**, 637 (1985), *ibid.* **C34**, 101 (1987).
7. E. Golowich and S. Pakvasa, *Phys. Rev.* **D51**, 1215 (1995); D. Atwood, B. Blok, and A. Soni, SLAC Report SLAC-PUB-6635 (1994) ; G. Eilam, A. Ioannissian, and R.R. Mendel, Technion Report PH-95-4 (1995).
8. A. Acker and S. Pakvasa, *Mod. Phys. Lett.* **A7**, 1219 (1992).
9. S. Pakvasa, in *CHARM2000 Workshop*, Fermilab, June 1994.
10. S. Davidson, D. Bailey, and B.A. Campbell, *Z. Phys.* **C61**, 613 (1994).
11. M. Derrick *et al.*, (ZEUS Collaboration), DESY Report 94-07 (1994).
12. W.-S. Hou, *Phys. Rev.* **D48**, 2342 (1993); P. Krawczyk and S. Pokorski, *Phys. Rev. Lett.* **60**, 182 (1988).
13. G. Blaylock, A. Seiden, and Y. Nir, Univ. of California Santa Cruz Report SCIPP 95/16 (1995); T. Liu, in *CHARM2000 Workshop*, Fermilab, June 1994.
14. A. Datta, *Z. Phys.* **C27**, 515 (1985).
15. G. Burdman in *CHARM2000 Workshop*, Fermilab, June 1994; J. Donoghue *et al.*, *Phys. Rev.* **D33**, 179 (1986).
16. H. Georgi, *Phys. Lett.* **B297**, 353 (1992); T. Ohl *et al.*, *Nucl. Phys.* **B403**, 605 (1993).
17. K.S. Babu *et al.*, *Phys. Lett.* **B205**, 540 (1988); T.G. Rizzo, *Int. J. Mod. Phys.* **A4**, 5401 (1989).
18. J.L. Hewett, *Phys. Rev. Lett.* **70**, 1045 (1993); V. Barger, J.L. Hewett, and R.J.N. Phillips, *Phys. Rev.* **D41**, 3421 (1990).
19. R. Ammar *et al.*, CLEO Collaboration, *Phys. Rev. Lett.* **71**, 674 (1993);
20. S. Pakvasa and H. Sugawara, *Phys. Lett.* **73B**, 61 (1978); T.P. Cheng and M. Sher, *Phys. Rev.* **D35**, 3484 (1987); L. Hall and S. Weinberg, *Phys. Rev.* **D48**, 979 (1993).
21. D. Schaile, in *27th International Conference on High Energy Physics*, Glasgow, Scotland, July 1994; U. Uwer in *30th Rencontres de Moriond: Electroweak Interactions and Unified Theories*, Meribel les Allures, France, March 1995; H. Neal (SLD Collaboration), *ibid.*
22. F. Abe *et al.*, (CDF Collaboration), FERMILAB-PUB-95-022-E (1995); S. Abachi *et al.*, (D0 Collaboration), FERMILAB-PUB-95-028-E (1995).
23. The ZFITTER package: D. Bardin *et al.*, *Z. Phys.* **C44**, 493 (1989); *Nucl. Phys.* **B351**, 1 (1991); *Phys. Lett.* **B255**, 290 (1991); CERN Report, CERN-TH-6443/92, 1992.
24. T.G. Rizzo, *Phys. Rev.* **D51**, 3811 (1995); G. Kopp *et al.*, *Z. Phys.* **C65**, 545 (1995).

25. For a review and original references, see, J.L. Hewett and T.G. Rizzo, *Phys. Rep.* **183**, 193 (1989); R.N. Mohapatra, *Unification and Supersymmetry*, (Springer, New York, 1986).